Hindawi
Mathematical Problems in Engineering
Volume 2020, Article ID 1849816, 9 pages
https://doi.org/10.1155/2020/1849816

Research Article

A Discrete Nonlinear Tracking-Differentiator and Its Application in Vibration Suppression of Maglev System

Zhiqiang Wang,[1,2] **Zhiqiang Long**,[1] **Yunde Xie**,[3] **Jingfang Ding**,[4,5] **Jie Luo**,[1] **and Xiaolong Li**[1]

[1]*Engineering Research Center of Maglev, National University of Defense Technology, Changsha, Hunan 410073, China*
[2]*Hunan Provincial Key Laboratory of Electromagnetic Levitation and Propulsion Technology, Changsha, Hunan 410073, China*
[3]*Beijing Enterprises Holding Maglev Technology Development Company Limited, Beijing 100000, China*
[4]*Laboratory of Networked Control Systems, Shenyang Institute of Automation, Chinese Academy of Sciences, Shenyang 110016, China*
[5]*University of Chinese Academy of Sciences, Beijing 100049, China*

Correspondence should be addressed to Yunde Xie; xieyd9999@163.com

Received 8 December 2019; Revised 1 March 2020; Accepted 5 March 2020; Published 19 June 2020

Academic Editor: Filippo Cacace

Vibration of the maglev train levitation system is harmful to riding comfort and safety. The signal processing method is effective in vibration control. In this paper, a novel kind of second-order nonlinear tracking differentiator is proposed and applied to suppress the vibration phenomenon. The switching curves of the second-order discrete time optimal control system are presented by the isochronous region method. A synthetic function is acquired depending on the cases whether a point in the phase plane can reach the switching curves within one sample step. The discrete form of tracking differentiator is constructed based on the position relationship between the state point and the characteristic curves. Numerical simulation shows that this discrete tracking differentiator can quickly track an input signal without overshoot and chattering and can produce a good differential signal. A test in a maglev test bench also demonstrates the effectiveness of the tracking differentiator in the suppression of the track-train vibration.

1. Introduction

Maglev train is a new type of modern railway transportation tool. Compared with the conventional wheel-rail train, it possesses the advantages of steady and comfortable riding, low noise, small turning radius, and strong climbing ability. The maglev train has a wide application prospect; the Changsha Maglev Express and the Beijing Maglev S1 are well welcomed by passengers. Making the train levitate above the track steadily is the foundation for the operation of the maglev train. To accomplish this purpose, it is necessary to gain the levitation gap of the train, vertical acceleration of the levitation electromagnet, the current of the electromagnet, and other information through the sensors as the feedback and then calculate the control output based on all the feedback. The quality of the sensor signals and corresponding signal processing technique play an important role in the performance of the levitation system.

To simplify the design of control system and to improve system performance, an effective way to acquire differential signal is of great importance. Tracking differentiator (TD) is firstly proposed for this purpose [1]. TD can also be used to design nonlinear PID controller, estimate parameters, and acquire differential information. Also, TD can be employed as a basic component of ADRC (auto disturbance rejection control) in charge of arranging transition process. Han proposed a discrete tracking differentiator based on second-order time optimal system. The differentiator can acquire the differential signal effectively, with the property of fast tracking input signal and no overshoot and chattering [2].

Lots of research studies are carried out about tracking differentiator [3–11]. Xie and Long [12] proposed a high accuracy fast TD, and this TD is used in signal detection in the maglev control system [13, 14]. Other applications of TD can be seen in [15–18].

Digital control systems are common in modern control engineering, which makes the study of discrete form controllers and signal processors valuable. For discrete form TD, the region of the linear zone needed in switching function has a nonignorable influence on TD's tracking and differential performance. Literature [2] uses the isochronous region method to specify the linear zone when time optimal control adopts nonextreme value; it presents the normal form of control synthetic function; however, the form is too complicated to be implemented in engineering practice. Another strategy, searching the boundary characteristic points which makes the time optimal control adopt nonextreme value and construct sectionwise linear function to avoid complicated computation, is used in this paper. Numerical simulation shows that this new form TD has the same advantage of the form in [2], and it can fast track input signal without overshoot and chattering and can acquire effective differential signal. However, the new form, which is a piecewise linear function, is much more simplified. The characteristic points are obtained in this strategy when the fastest control function adopts nonoptimal value based on the isochronous region method, and then a piecewise fastest control function is constructed based on the characteristics of the fastest control system.

The remainder of this paper is organized as follows. First, a description about maglev train levitation system is given in Section 2, and then in Section 3, a detailed procedure of how this tracking differentiator is derived is given. In Section 4, simulation results are given to verify the effectiveness of this tracking differentiator in suppression of maglev train vibration, and Section 5 concludes this paper.

2. Maglev Train Levitation System

Figure 1 is a photo of Changsha Maglev Express, which connects the airport and the railway station. The length of Changsha Maglev Express operation line is 18 km, which is the longest ever for mid-low speed maglev train.

The interactions between the electromagnets and the tracks play a key role in maglev train. The structure and schematic diagram of maglev train levitation system can be seen in Figures 2(a) and 2(b), respectively. A fundamental maglev system consists of electromagnet, sensor, and controller. In the research of maglev trains, since the mechanical decoupling of the suspension modules on both sides has been achieved by the bogie, a single point is usually used as the research object of the suspension control system. We simplify the single-point suspension system into the model shown in Figure 2(b) and make the following assumptions:

(i) Magnetic leakage and edge effects are ignored, and the magnetic flux is considered to be evenly distributed on the air gap.

(ii) The magnetic resistances of guide rails, iron cores, and plates are ignored.

Figure 1: Photo of Changsha Maglev Express.

(iii) It is considered that the levitation force provided by the electromagnet is concentrated on the geometric center and the geometric center of the electromagnet coincides with the center of mass.

(iv) It is believed that there is no dislocation between the magnetic pole surface and the guide rail, that is, the electromagnet has no rolling movement relative to the track, but only vertical movement. The force of the air spring on the electromagnet is also vertical.

2.1. Reference Coordinates. When the interference of track irregularity is considered, a new absolute reference surface is needed. In Figure 2(b), $h(t)$ represents the displacement of the track relative to the reference plane, $c(t)$ is the absolute displacement of the electromagnet relative to the absolute reference plane, and $z(t)$ is the gap between the track and the electromagnet.

$$c(t) = h(t) + z(t). \tag{1}$$

2.2. Kinetic Equation. From Newton's second law, the kinetic equation can be obtained as:

$$m\ddot{c} = (m + M)g - F(i, z) + \Delta F, \tag{2}$$

where m is the equivalent mass of electromagnet, M is the equivalent mass of carriage, $F(i, z)$ is the electromagnetic force, i is the current in the electromagnet coil, ΔF is the increment of the force exerted on the bogie by the air spring relative to the static state, and its acting point is the installation position of the air spring. Because the frequency of the air spring itself is far lower than the natural frequency of the suspension system, in normal circumstances, the displacement of the suspension module relative to its balance position is also very small due to the control function. Therefore, compared with the electromagnetic force provided by the electromagnet, ΔF can be ignored.

2.3. Electrical Equation

$$u(t) = Ri(t) + \frac{\mu_0 N^2 A}{2} \cdot \frac{\dot{i}(t)}{z(t)} - \frac{\mu_0 N^2 A i(t)}{2} \frac{\dot{z}(t)}{[z(t)]^2}, \tag{3}$$

where $u(t)$ is the control voltage applied at both ends of the coil windings, R is the coil impedance, N is the number of

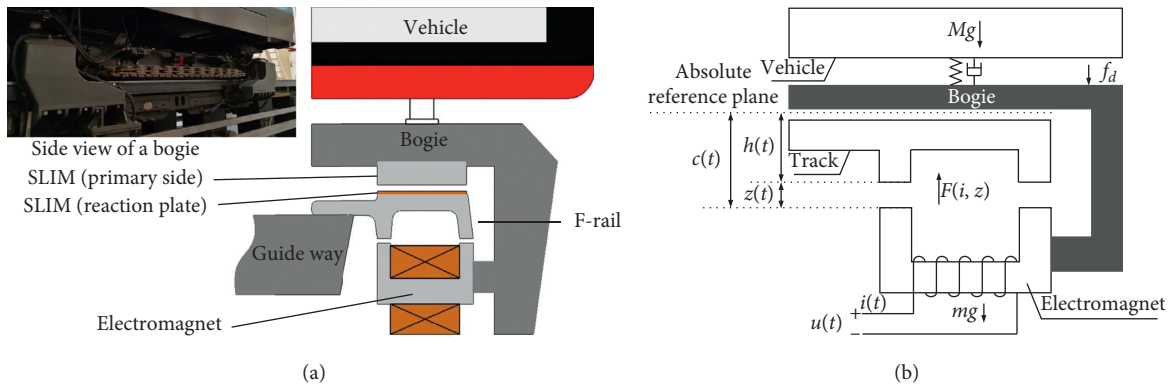

FIGURE 2: Maglev train levitation system. (a) Structure of maglev train levitation system. (b) Schematic diagram of maglev train levitation system.

turns of the coil windings, A is the pole area of the electromagnet, and μ_0 is the vacuum permeability.

2.4. Electromagnetic Force Equation

$$F(i,z) = \frac{\mu_0 N^2 A}{4}\left[\frac{i(t)}{z(t)}\right]^2. \tag{4}$$

2.5. Boundary Condition

.

$$(m+M)g = F(i_0,z_0) = \frac{\mu_0 N^2 A}{4}\left[\frac{i_0}{z_0}\right]^2, \qquad c_0 = h_0 + z_0, \tag{5}$$

where i_0 and z_0 are the values of the coil current and gap in steady state, respectively, and c_0 and h_0 are also the initial values of the track and electromagnet relative to the reference plane in steady state.

Making a Taylor expansion of the above model at the boundary equilibrium point and denoting $K = (\mu_0 A N^2/4)$, a linearized model can be acquired.

$$\begin{cases} m\Delta\ddot{c}(t) = \dfrac{2Ki_0^2}{z_0^3}\Delta z(t) - \dfrac{2Ki_0}{z_0^2}\Delta i(t), \\ \Delta u(t) = R\Delta i(t) + \dfrac{2K}{z_0}\Delta\dot{i}(t) - \dfrac{2Ki_0}{z_0^2}\Delta\dot{z}(t), \\ \Delta c(t) = \Delta h(t) + \Delta z(t). \end{cases} \tag{6}$$

Since electromagnets fluctuate in a small range near the equilibrium point, the $\dot{z}$ term in the electrical equation can be ignored, and the inductance can be approximated as $(2K/z0)$. Taking the state variable as $X = (x_1, x_2, x_3)^T = (\Delta z, \Delta\dot{c}, \Delta i)^T$, the state space representation of the maglev system can be obtained as follows:

$$\dot{X} = \begin{bmatrix} 0 & 1 & 0 \\ \dfrac{2Ki_0^2}{z_0^3 m} & 0 & -\dfrac{2Ki_0}{z_0^2 m} \\ 0 & \dfrac{i_0}{z_0} & -\dfrac{Rz_0}{2K} \end{bmatrix} X + \begin{bmatrix} 0 \\ 0 \\ \dfrac{z_0}{2K} \end{bmatrix}\Delta u + \begin{bmatrix} -1 \\ 0 \\ -\dfrac{i_0}{z_0} \end{bmatrix}\Delta\dot{h}. \tag{7}$$

3. Second-Order Discrete System Control Synthesis Function

3.1. Preliminaries. For a discrete form double integral time optimal control (TOC) system:

$$\begin{bmatrix} x_1(k+1) \\ x_2(k+1) \end{bmatrix} = \begin{bmatrix} 1 & h \\ 0 & 1 \end{bmatrix}\begin{bmatrix} x_1(k) \\ x_2(k) \end{bmatrix} + \begin{bmatrix} 0 \\ h \end{bmatrix}\cdot u(k), \quad |u(k)| \le r, k = 0,1,2,\ldots, \tag{8}$$

where $X(k) = [x_1(k), x_2(k)]^T \in \mathcal{R}^2$ is the state variable, $u(k) \in \mathcal{R}$ is the control variable with constrained amplitude $r \in \mathcal{R}^+$, and $h \in \mathcal{R}^+$ is the sample step; the corresponding state space form expression can be obtained as:

$$X(k+1) = AX(k) + Bu(k), \tag{9}$$

in which $A = \begin{pmatrix} 1 & h \\ 0 & 1 \end{pmatrix}, B = \begin{pmatrix} 0 \\ h \end{pmatrix}$. A universal solution of equation (9) with initial value of $X(0)$ is:

$$X(k+1) = A^{k+1}X(0) + \sum_{i=0}^{k} A^{k-i}Bu(i). \tag{10}$$

If after $k+1$ steps, the state point $M_{k+1} = X(k+1)$ finally arrives at the origin in the phase plane, that is, $X(k+1) = [0,0]^T$, then from (11), the mathematical condition the initial point follows is obtained as:

$$X(0) = -\sum_{i=0}^{k} A^{-i-1} B u(i). \tag{11}$$

Substituting A and B into (11) yields:

$$X(0) = \sum_{i=0}^{k} \begin{pmatrix} (i+1)h^2 \\ -h \end{pmatrix} \cdot u(i). \tag{12}$$

From optimal control theory for continuous system, any point in the phase plane needs at most one switch before reaching at the origin along the optimal trajectory. For continuous system, the switching is finished at instance with no delay. However, for discrete control system, the switching process takes place within a sample step h after the state point passes the switching line with the continuous control law, which is also called a "bang-bang" control strategy. Define those points which can converge to the origin when $u = +r$ or $u = -r$ always as $\{a_{+k}\}$ or $\{a_{-k}\}$. Define those points which can converge to the origin when $u = -r$ first then $u = +r$ always or $u = +r$ first then $u = -r$ always as $\{b_{+k}\}$ or $\{b_{-k}\}$, $k \geq 2$. Define those points which can converge to the origin when $u = 0$ first then $u = +r$ or $u = -r$ always as $\{c_{+k}\}$ or $\{c_{-k}\}$, $k \geq 2$. Define the curve constituted by $\{a_{+k}\}$ as Γ_A^+, by $\{a_{-k}\}$ as Γ_A^-, by $\{b_{+k}\}$ as Γ_B^+, by $\{b_{-k}\}$ as Γ_B^-, by $\{c_{+k}\}$ as Γ_C^+, and by $\{c_{-k}\}$ as Γ_C^-. The next task is to determine the mathematical descriptions of these boundary lines.

3.2. Determination of the Boundaries. In this part, the mathematical descriptions for the boundaries mentioned above are determined in detail. Firstly, the boundary $\Gamma_A = \Gamma_A^+ \cup \Gamma_A^-$ is determined. Suppose that a state point reaches the origin in $k+1$ steps, that is, $X(k+1) = 0$, and $u(i) = +r, i = 0, 1, \ldots, k$. From (12),

$$X(0) = r \cdot \sum_{i=0}^{k} \begin{pmatrix} (i+1)h^2 \\ -h \end{pmatrix}. \tag{13}$$

Then,

$$\begin{aligned} x_1(0) &= rh^2 \sum_{i=0}^{k} (i+1) = rh^2 \left(\frac{k^2}{2} + \frac{3k}{2} + 1 \right), \\ x_2(0) &= -rh(k+1) < 0. \end{aligned} \tag{14}$$

For simplicity, denote $x_1(0)$ as x_1 and $x_2(0)$ as x_2; then, the following equation can be derived:

$$x_1 = \frac{x_2^2}{2r} - \frac{1}{2} h \cdot x_2, \quad x_2 < 0. \tag{15}$$

Formula (15) is the mathematical description of Γ_A^+. In the same way, the mathematical description of Γ_A^- can be derived as follows:

$$x_1 = -\frac{x_2^2}{2r} - \frac{1}{2} h \cdot x_2, \quad x_2 > 0. \tag{16}$$

Formulas (15) and (16) can be combined into one unity formula as follows:

$$\Gamma_A(x_1, x_2)\colon\ x_1 + \frac{x_2 |x_2|}{2r} + \frac{1}{2} h \cdot x_2 = 0. \tag{17}$$

Then, the boundary line $\Gamma_B = \Gamma_B^+ \cup \Gamma_B^-$ is to be determined. For state points $\{b_{+k}\}$, there are $X(k+1) = 0$, and $u(0) = -r$, $u(i) = +r$, $i = 1, 2, \ldots, k$. Then, the following relationships can be obtained:

$$x_1(0) = -rh^2 + r \sum_{i=1}^{k} (i+1)h^2 = rh^2 \left(\frac{k^2}{2} + \frac{3k}{2} - 1 \right), \tag{18}$$

$$x_2(0) = -rh(k-1). \tag{19}$$

For simplicity, denote $x_1(0)$ as x_1 and $x_2(0)$ as x_2. From formulas (18) and (19), relation (20) can be derived.

$$\begin{aligned} x_1 &= \frac{x_2^2}{2r} - \frac{5}{2} h x_2 + h^2 r, \\ x_1 + h x_2 &= \frac{1}{2} r h^2 k(k+1) > 0. \end{aligned} \tag{20}$$

Formula (20) is the mathematical description of Γ_B^+; in the same way, the mathematical description of Γ_B^- is as follows:

$$\begin{aligned} x_1 &= -\frac{x_2^2}{2r} - \frac{5}{2} h x_2 - h^2 r, \\ x_1 + h x_2 &< 0. \end{aligned} \tag{21}$$

Combining (20) and (21), the description of $\Gamma_B = \Gamma_B^+ \cup \Gamma_B^-$ is as follows:

$$x_1 - s \cdot \frac{x_2^2}{2r} + \frac{5}{2} h x_2 - s \cdot h^2 r = 0, \quad s = \operatorname{sgn}(x_1 + h x_2). \tag{22}$$

Furthermore, the boundary $\Gamma_C = \Gamma_C^+ \cup \Gamma_C^-$ is to be determined. For state points $\{c_{+k}\}$, there are $X(k+1) = 0$, $u(0) = 0$, $u(i) = +r$, $i = 1, 2, \ldots, k$. For state points $\{c_{-k}\}$, there are $X(k+1) = 0$, $u(0) = 0$, $u(i) = -r$, $i = 1, 2, \ldots, k$. For simplicity, denote $x_1(0)$ as x_1 and $x_2(0)$ as x_2, and the mathematical description of $\Gamma_C = \Gamma_C^+ \cup \Gamma_C^-$ can be derived in the same way:

$$\Gamma_C(x_1, x_2)\colon\ x_1 + \frac{x_2 |x_2|}{2r} + \frac{3}{2} h \cdot x_2 = 0. \tag{23}$$

Then, all boundaries of region Ω and control characteristic lines are determined by (17), (22), and (23). The boundary curves can now been obtained as shown in Figure 3.

3.3. Determination of Control Synthesis Function. Linear zone Ω (the area between Γ_A and Γ_B) and its boundary lines have already been determined in the above part. For any state point $M(x_1, x_2)$ in the phase plane, if $M(x_1, x_2) \notin \Omega$, then control value u adopts an extremum; if $M(x_1, x_2) \in \Omega$, u changes according to some linear law in the range of $[-r, +r]$.

As shown in Figure 4, any point $M(x_1, x_2)$ in the phase place converges to the origin going through the switching line at most once, and that sign-changing process takes place

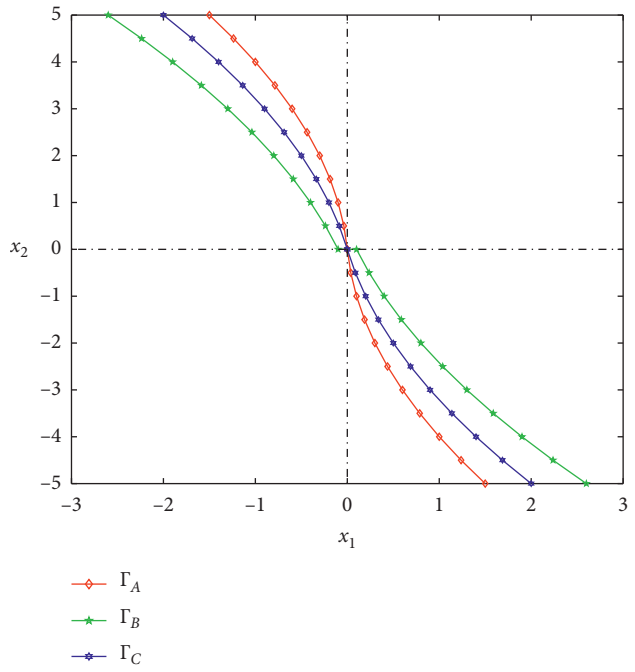

Figure 3: Boundaries of linear regions.

in linear zone Ω at the adjacent of switching line Γ_A. One idea is to confirm the steps k it needs to reach the switching line Γ_A. If k is no less than 1, then it means $M \notin \Omega$. Under this condition, u adopts an extremum $u = +r\,(-r)$. Otherwise, u adopts some particular value and $|u| < r$. Suppose that M is above the switching line Γ_A and after k steps it reaches to the point $\widehat{M}(\widehat{x}_1, \widehat{x}_2) \in \Gamma_A$. From (10), $X(k+1) = A^{k+1}X(0) + \sum_{i=0}^{k} A^{k-i}Bu(i)$, $u(i) = -r, i = 0, 1, \ldots, k$. That is,

$$\begin{cases} \widehat{x}_1 = x_1 + (k+1)hx_2 - \dfrac{1}{2}rh^2k(k+1), \\ \widehat{x}_2 = x_2 - (k+1)rh, \\ \widehat{x}_1 - \dfrac{\widehat{x}_2^2}{2r} + \dfrac{1}{2}h\widehat{x}_2 = 0, \quad \widehat{x}_2 < 0. \end{cases} \tag{24}$$

The value of k can be obtained by solving these equations as $k = -1 + (x_2/rh) \pm (1/h)\sqrt{(1/r)(x_1 + (x_2^2/2r) + (1/2)hx_2)}$. Since in (24), $\widehat{x}_2 < 0$and $k > 0$, $k = -1 + (x_2/rh) + (1/h)\sqrt{(1/r)(x_1 + (x_2^2/2r) + (1/2)hx_2)}$. Since $x_2^2 \geq x_2|x_2|$ and $x_1 + (x_2^2/2r) + (1/2)hx_2 \geq x_1 + (x_2|x_2|/2r) + (1/2)hx_2 > 0$, k can be further rewritten as follows:

$$k = -1 + \frac{x_2}{rh} + \frac{1}{h}\sqrt{\frac{1}{r}\left|x_1 + \frac{x_2^2}{2r} + \frac{1}{2}hx_2\right|} > 0. \tag{25}$$

In the same way, the steps k it takes for point M below switching line Γ_A to reach the switching line can be derived as follows:

$$k = -1 - \frac{x_2}{rh} + \frac{1}{h}\sqrt{\frac{1}{r}\left|x_1 - \frac{x_2^2}{2r} + \frac{1}{2}hx_2\right|} > 0. \tag{26}$$

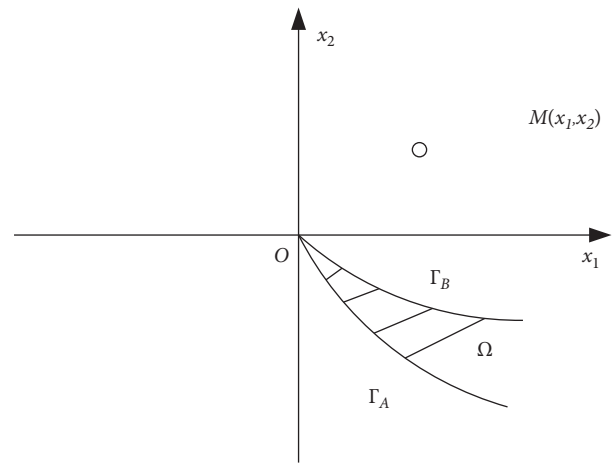

Figure 4: Boundaries Γ_A and Γ_B for linear region Ω.

These two conditions can be combined into a unified one:

$$\begin{aligned} \widehat{s} &= \operatorname{sgn}\left(x_1 + \frac{x_2|x_2|}{2r} + \frac{1}{2}hx_2\right), \\ k &= -1 + \frac{x_2\widehat{s}}{rh} + \frac{1}{h}\sqrt{\frac{1}{r}\left|x_1 + \frac{x_2^2}{2r}\widehat{s} + \frac{1}{2}hx_2\right|} > 0. \end{aligned} \tag{27}$$

If $k \geq 1$, it is obvious that $u = -r\widehat{s}$. If $k < 1$, $M(x_1, x_2)$ can reach Γ_A within one step. Under this condition, a proper control value u is needed to make $M(x_1, x_2)$ arrive at Γ_A exactly. Suppose at control value $u = \widehat{u}$, $M(x_1, x_2)$ will arrive at $\widehat{M}(\widehat{x}_1, \widehat{x}_2)$, then it will reach the origin along Γ_A^+ under $u = +r$ or along Γ_A^- under $u = -r$. From (12),

$$\begin{cases} X(0) = \displaystyle\sum_{i=0}^{k}\begin{pmatrix} (i+1)h^2 \\ -h \end{pmatrix} \cdot u(i), \\ u(0) = \widehat{u}, \quad u(i) = r \cdot \widehat{s}, \\ X(0) = [x_1, x_2]^T. \end{cases} \tag{28}$$

Then, the following relationship can be derived:

$$\begin{cases} (x_1/h) = h\widehat{u} + \widehat{s}rh\left[\dfrac{1}{2}k^2 + \dfrac{3}{2}k\right], \\ (x_2/h) = -\widehat{u} - \widehat{s}rk. \end{cases} \tag{29}$$

The solution of $\widehat{u}$ in terms of x_1 and x_2 can be also derived as follows:

$$\widehat{u} = -\frac{x_2}{h} + \frac{r}{2}\left(\widehat{s} \pm \sqrt{1 + \frac{8\widehat{s}}{rh}\left(x_2 + \frac{x_1}{h}\right)}\right). \tag{30}$$

Since $x_1 + hx_2 = (1/2)\widehat{s}rh^2k(k+1)$, $x_1 + hx_2$ has the same sign with $\widehat{s}$. Then, the following solution is also true: $\widehat{u} = -(x_2/h) + (r/2)(\widehat{s} \pm \sqrt{1 + (8/rh)|(x_2 + (x_1/h))|})$. This form can further be rewritten as:

$$\widehat{u} = -r\widehat{s}u_a, \tag{31}$$

in which:

$$u_a = -\frac{1}{2} + \frac{x_2\hat{s}}{rh} \pm \frac{1}{2}\hat{s}\sqrt{1 + \frac{8}{rh}\left|x_2 + \frac{x_1}{h}\right|}. \tag{32}$$

One root of (32) is to be excluded. From (28) and (29), $-(2k+1)\hat{s} = \pm\sqrt{1 + (8/rh)|x_1 + (x_2/h)|}$, and the sign of the square root is related with the sign of $\hat{s}$, so (32) can be written as:

$$u_a = -\frac{1}{2} + \frac{x_2\hat{s}}{rh} + \frac{1}{2}\sqrt{1 + \frac{8}{rh}\left|x_2 + \frac{x_1}{h}\right|}. \tag{33}$$

If $M(x_1, x_2)$ is in the first quadrant or the third quadrant, since it is not within Ω, then:

$$u = -r \cdot \operatorname{sgn}(x_1), \quad x_1 \cdot x_2 > 0. \tag{34}$$

If $M(x_1, x_2)$ can arrive at the origin in two steps, every state and control value must satisfy (8), which are the following relationships:

$$\begin{cases} x_1(1) = x_1(0) + hx_2(0), \\ x_2(1) = x_2(0) + hu(0), \\ x_1(2) = x_1(1) + hx_2(1), \\ x_2(2) = x_2(1) + hu(1). \end{cases} \tag{35}$$

Setting $x_1(2) = 0$ and $x_2(2) = 0$, (35) can be written in matrix form as:

$$\begin{pmatrix} 1 & h & 0 & 0 \\ 0 & 1 & 0 & h \\ 1 & 0 & 0 & h \\ 0 & 1 & -h & 0 \end{pmatrix} \cdot \begin{pmatrix} x_1(1) \\ x_2(1) \\ u(0) \\ u(1) \end{pmatrix} = \begin{pmatrix} 0 \\ 0 \\ x_1(0) \\ x_2(0) \end{pmatrix}. \tag{36}$$

Then,

$$\begin{cases} u(0) = -\dfrac{x_1(0) + 2hx_2(0)}{h^2}, \\ \\ u(1) = -\dfrac{x_1(1) + hx_2(1)}{h^2}. \end{cases} \tag{37}$$

There is no harm in defining the control synthesis function as $u = \text{fast}(x_1, x_2, r, h)$, and based on all these analyses, a time optimal synthesis function can be obtained by the following theorem.

Theorem 1. *For an arbitrary $M(x_1, x_2)$ in the phase plane, it can reach the origin quick under the fastest synthesis function $u = fast(x_1, x_2, r, h)$ obtained in the following procedure:*

(1) If $|x_1 + hx_2| > h^2 r$, $M(x_1, x_2)$ cannot arrive at the origin within two steps, else jump to (5).

(2) If $x_1 \cdot x_2 > 0$, $M \notin \Omega$, $u = -r \cdot sgn(x_1)$.

(3) Calculate the number of steps it needs for $M(x_1, x_2)$ to reach the line Γ_A $k = -1 + (x_2 \quad \hat{s}/rh) + (1/h)\sqrt{(1/r)|x_1 + (x_2^2/2r)\hat{s} + (1/2)hx_2|} > 0$, $\hat{s} = \operatorname{sgn}(x_1 + ((x_2|x_2|)/2r) + (1/2)hx_2)$. If $k > 1$, $M \notin \Omega$, $u = -r\hat{s}$.

(4) If M can reach Γ_A in one step, $u_a = -(1/2) + (x_2\hat{s}/rh) + (1/2)\sqrt{1 + (8/rh)|x_2 + (x_1/h)|}$, $u = -r\hat{s}u_a$.

(5) M can reach the origin in two steps, $u = -(x_1 + 2hx_2/h^2)$.

(6) The end.

A nonlinear discrete tracking differentiator based on the previous mentioned synthesis function is described as follows. For a given signal sequence $\{v(k), k = 1, 2, \ldots\}$, apply

$$\begin{cases} u(k) = \text{fast}(x_1(k) - v(k), x_2(k), r, c_0 \cdot h), \\ x_1(k+1) = x_1(k) + h \cdot x_2(k), \\ x_2(k+1) = x_2(k) + h \cdot u(k). \end{cases} \tag{38}$$

Then, $x_1(k)$ approaches $v(k)$ and $x_2(k)$ approaches the differential of $v(k)$. In (38), c_0 is named as filtering coefficient and h is named as sampling steps. The tracking differentiator above is a piecewise linear function, its structure is clearer, computation is simpler, and the fastest trajectories are shown in Figure 5.

From Figure 5, when the trajectory enters Ω, it may fall in the area bounded by Γ_A and Γ_C or Γ_C and Γ_B; then, under proper control value according to fast$(\cdot)$ algorithm, the trajectory will move to the origin along Γ_A.

4. Numerical Simulations of Discrete Tracking Differentiator

In this part, numerical simulations are given to verify the effectiveness of the proposed tracking differentiator. Firstly, a simulation test for given signals are performed, then a test in maglev test bench is done.

4.1. Given Signal Tests. For a given signal sequence $\{v(k), k = 1, 2, \ldots\}$, a tracking differentiator in the form of (38) is constructed and then the tracking numerical simulation results and differential numerical simulation results of a sinuous signal and a square wave signal are given.

4.1.1. Sinuous Test Signal

$$v(k) = \sin\left(\frac{k\pi}{50}\right), \quad k = 0, 1, 2, \ldots. \tag{39}$$

4.1.2. Square Wave Signal

$$v(k) = \begin{cases} +1, & 100m < k \le (100m + 50), \\ -1, & 100m + 50 < k \le 100(m+1), \ m = 0, 1, 2, \ldots. \end{cases} \tag{40}$$

The simulation result for a sinuous test signal is shown in Figure 6 while the simulation result for a square wave signal is shown in Figure 7. Both simulation results show that the above tracking differentiator can track the sinuous signal and square wave signal without overshoot and the differential of the given signal can be acquired properly.

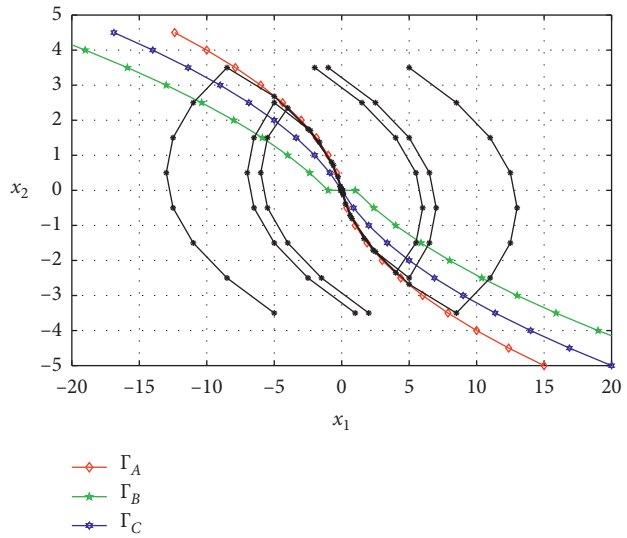

Figure 5: Switching curves, boundary lines, and fastest trajectories.

4.2. Application in Vibration Suppression of Maglev System. Vibration is a vital problem for maglev train which originates from the elastic property of the track and the coupling of maglev train and track [19, 20]. Many research studies have been carried out about the suppression methods of train-track coupling vibration. But most of them are too complicated and rely heavily on the precise system model. It is verified in practice that a signal processing method is sometimes simple and effective. The common feedback control method for levitation control in maglev system is as follows:

$$u_0 = K_z z + K_c i + K_v \int a\,\mathrm{d}t + K_i \int (z - z_{\mathrm{ref}})\mathrm{d}t, \qquad (41)$$

where z is the levitation gap, i is the current through the electromagnet windings, a is the acceleration of the electromagnet, and z_{ref} is the reference gap value. K_z, K_c, K_v, and K_i are corresponding feedback gain and their values can be obtained via pole placement or the LQR method. This control law works well under the assumption that the track is rigid. However, the track itself vibrates under the effect of electromagnet force, and levitation gap is the difference between the displacement of track and the displacement of electromagnet. To get rid of this coupling, the differential of levitation gap signal can be used to restrain the coupling vibration. Considering this, a tracking differentiator based vibration suppression control scheme is designed in Figure 8. In this scheme, the feedback of gap differential is added to the control output, which results in the following:

$$\mathrm{u}_1 = K_z z + K_b \frac{\mathrm{d}z}{\mathrm{d}t} + K_c i + \mathrm{K}_v \int a\,\mathrm{d}t + K_i \int (z - z_{\mathrm{ref}})\mathrm{d}t, \qquad (42)$$

where signal $(\mathrm{d}z/\mathrm{d}t)$ is obtained from the tracking differentiator and K_b is the corresponding differential coefficient.

To verify this, a simulation on a maglev test bench described by the model of (6) is made with the results shown in Figure 9. At first, the maglev system works under control law (41), then from $t = 4$ s to $t = 6$ s, control law (42) is applied with the differential signal obtained from an ordinary differentiator, and after $t = 6$ s, tracking differentiator is applied for extracting differential from noised signal. Their performances are labelled separately in different colors in Figure 9, with the red curve representing the control performance by control law (41), the blue curve representing the control performance by control law (42) without tracking

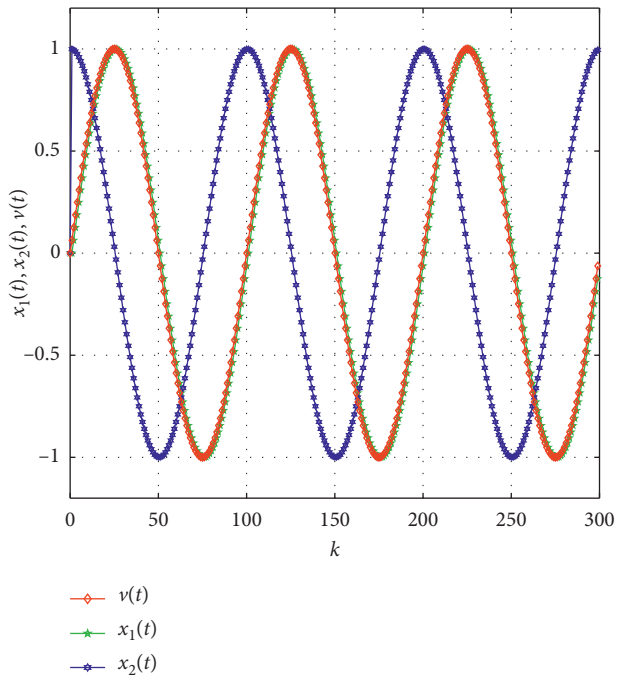

Figure 6: Tracking and differential of sinuous signal.

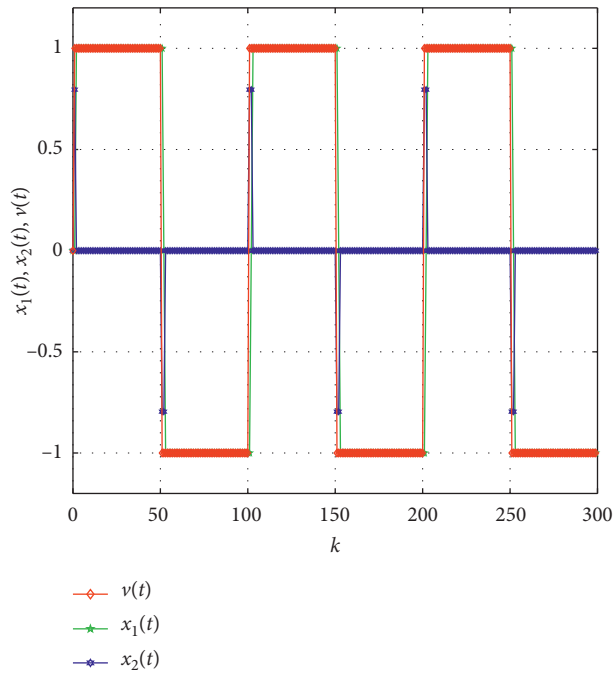

Figure 7: Tracking and differential of square wave signal.

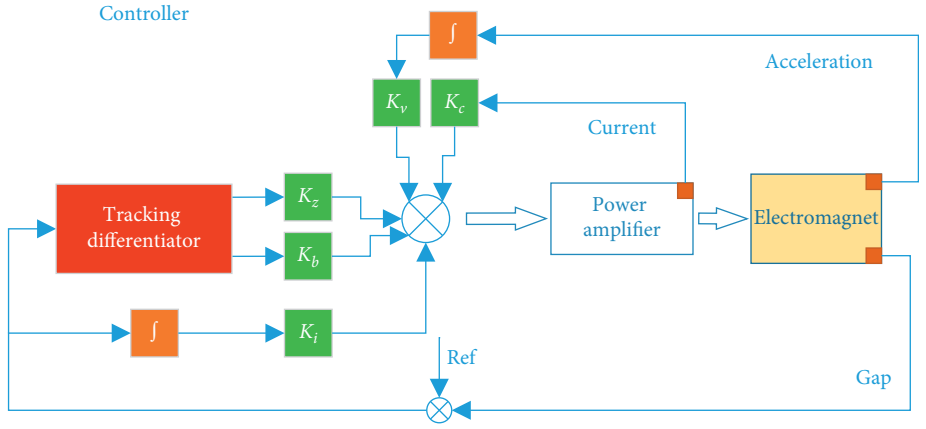

Figure 8: Levitation control diagram with tracking differentiator for vibration suppression.

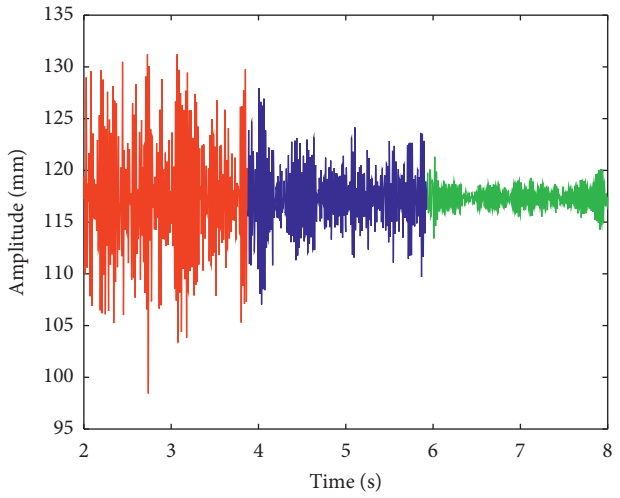

Figure 9: Vibration suppression performance using tracking differentiator.

differentiator, and the green curve representing the control performance by control law (42) with the proposed tracking differentiator. Even though control scheme (42) has a better vibration suppression ability, during $t = 4$ s to $t = 6$ s, the ordinary differentiator amplified the noise in the signal which makes the vibration still strong, whereas the tracking differentiator can suppress the noise more effectively. From this comparative simulation result, it can be seen that the proposed tracking differentiator is effective and superior in suppressing vibration.

5. Conclusion

A discrete tracking differentiator is constructed by discrete system fastest control synthesis function, the boundary that control value adopts non-extreme value and the areas in which control value changes linearly are obtained. The fastest system control synthesis function is obtained by regionwise linearization. Compared with other types of tracking differentiator, the computation is simple and its performance is as good as nonlinear tracking differentiator. Numerical simulation and experiment results show that this new type of tracking differentiator has good performance in tracking, differentiating, and eliminating fluttering.

Data Availability

Data sharing is not applicable to this article as all datasets are hypothetical during the current study.

Conflicts of Interest

The authors declare that they have no conflicts of interest.

Acknowledgments

This study was supported by the National Key Technology R&D Program of China (nos 2016YFB1200601 and 2016YFB1200602).

References

[1] H. J.-Q. W. Wei, "Nonlinear tracking-differentiator," *Journal of Systems Science and Mathematical Sciences*, vol. 2, p. 11, 1994.

[2] H. Jinqing and Y. Lulin, "The discrete form of tracking-differentiator," *Aournal of Systems IciTnce and Mathematical Sciences*, vol. 3, p. 2, 1999.

[3] H. Jingqing, "The improvement of PID control law by using nonlinearity," *Information and Control*, vol. 6, 1995.

[4] H. Jingqing, "Nonlinear PID controller," *Acta Automatica Sinica*, vol. 20, no. 4, pp. 487–490, 1994.

[5] C. Chang, W. Chaozhu, and H. Jingqpng, "A new approach to estimate the moving parameters for maneuvering objects," *Journal of Astronautics*, vol. 16, no. 1, pp. 30–34, 1995.

[6] W.-G. Zhang and J.-Q. Han, "The application of tracking differentiator in allocation of zero," *Actc Automatici Sinica*, vol. 27, no. 5, pp. 724–727, 2001.

[7] J. ean, "From PID to active disturbance rejection control," *IEEE Transactions on Industrial Electronics*, vol. 56, no. 3, pp. 900–906, 2009.

[8] Y. Hvang and W. Zhang, "Development of active disturbance rejection controller," *Control Theory & Applications*, vol. 19, no. 4, pp. 485–492, 2002.

[9] X.-H. Wang, N.-Q. Chei, and Z.-Z. Yuav, "Nonlinear tracking-differentiator with high speed in whole course,"

Control Theory & Applications, vol. 20, no. 6, pp. 875–878, 2003.

[10] L.-Q. Wu and J.-Q. Han, "Active disturbance rejection controller scheme for the linear inverted pendulum," *Control Theory & Applications*, vol. 21, no. 5, pp. 665–669, 2004.

[11] M. Zhang and J. Wu, "Control system of renewable energy connected grid based on the auto-disturbances rejection control technology," *Control Theory & Applications*, vol. 22, no. 4, pp. 583–587, 2005.

[12] Y.-d. Xie and Z.-q. Long, "A high-speed nonlinear discrete tracking-differentiator with high precision," *Control Theory & Applications*, vol. 26, no. 2, pp. 127–132, 2009.

[13] Z.-z. Zhang, L.-h. She, L.-l. Zwang, and X.-l. Li, "Damp signal acquiring and fusing technology for middle-low speed permanent-electro maglev trains," *Journal of the China Railway Society*, vol. 4, p. 8, 2011.

[14] X. Song, L. Zhiqiang, H. Ning, and C. Wensen, "A high precision position sensor design and its signal processing algorithm for Maglev train," *Sensors*, vol. 12, no. 5, p. 5, 2012.

[15] J. S.-t. H. Zhong-sheng, "An improved model-free adaptive control for a class of nonlinear large-lag system," *Control Theory & Applications*, vol. 4, p. 8, 2008.

[16] Y. Guo, W. Wu, and K. Tang, "A new inertial aid method for high dynamic compass signal tracking based on a nonlinear tracking differentiator," *Sensors*, vol. 12, no. 6, pp. 7634–7647, 2012.

[17] Y. Zhou, Q.-L. Wang, and D.-H. Qiu, "Cascade form of tracking differentiator with high-order indiscrimination degree," *Transactions of Beijing Institute of Technology*, vol. 31, no. 9, pp. 1058–1061, 2011.

[18] A. Xiong and Y. Fan, "Application if a nonlinear velocity estimator in photoelectronic tracking system," *Electronics Optics & Control*, vol. 11015 pages, 2010.

[19] J. Li, J. Li, D. Zhou, P. Cui, L. Wang, and P. Yu, "The active control of maglev stationary self-excited vibration with a virtual energy harvester," *IEEE Transactions on Industrial Electronics*, vol. 62, no. 5, pp. 2942–2951, 2015.

[20] D. Zhou, P. Yu, L. Wang, and J. Li, "An adaptive vibration control method to suppress the vibration of the maglev train caused by track irregularities," *Journal of Sound and Vibration*, vol. 408, pp. 331–350, 2017.